Supporting Information

Supplementary Methods

1. Physical characterizations

X-ray diffraction (XRD) testing is a common material characterization method used to analyse the crystalline structure and lattice constants of materials. It is defined as a structural analysis method in which a beam of high-energy X-rays is irradiated onto the sample, and the spatial distribution of atoms within the material is analysed by measuring the direction and intensity of X-rays scattered by the sample. The XRD testing in this work was performed using a Bruker AXS D8 ADVANCE (Bruker, Germany) with Cu Kα radiation (wavelength of 1.5418 Å). The samples were tested under continuous scanning conditions over a range of 5° to 90° at a scanning speed of 5° min^{-1}. This technique was primarily used for the qualitative analysis and trace detection of catalysts.

Scanning electron microscopy (SEM) is primarily used to observe the microscopic morphology of samples. The working principle of SEM relies on the surface physical properties of materials for microscopic imaging. SEM offers several advantages: first, a high magnification range adjustable from 2 to 200,000 times; second, the ability to capture the real three-dimensional structure of material surfaces; third, a simple sample preparation process. The SEM equipment used in this work was a Hitachi SU8010 (model 2012522201, Hitachi, Japan). The sample preparation process for SEM was as follows: an appropriate amount of catalyst was dispersed uniformly in ethanol. A small amount of the solution was dropped onto a silicon wafer, followed by gold sputtering to enhance the electrical conductivity of the material.

Transmission electron microscopy (TEM) is primarily used for observing sub microscopic structures with dimensions smaller than 0.2 μm. TEM employs an electron beam with a wavelength shorter than that of visible light as the light source. The main

principle involves projecting a focused and accelerated electron beam onto the surface of an ultrathin sample, where electrons collide with atoms in the sample, leading to scattering. The magnitude of the scattering angle is ultimately presented as an image with varying brightness, from which information about the material's density, thickness, and other related properties can be inferred. The TEM used in this study was a Tecnai G2 F30 manufactured by FEI Company, the Netherlands. The sample preparation process for TEM was as follows: an appropriate amount of catalyst was dispersed uniformly in ethanol, and a small amount of the solution was dropped onto a double-layer copper grid.

X-ray photoelectron spectroscopy (XPS) operates on the principle of irradiating a sample with monochromatic light, inducing photoionization to generate electrons. These electrons migrate to the material surface, overcome the work function, and are emitted, after which an energy analyser measures the kinetic energy of the photoelectrons to produce XPS spectra. XPS is primarily used for qualitative and semiquantitative analysis. Qualitative analysis identifies atomic oxidation states, atomic charges, and functional groups based on elemental chemical shifts, while semiquantitative analysis determines the surface content of specific elements, including their different oxidation states-by evaluating the intensity of photoelectrons at specific energies. The XPS instrument used in this study was a Thermo Scientific K-Alpha (model XN20210102).

2. Electrochemical measurements

Preparation of the working electrode: A rotating disk electrode (diameter of 5 mm) was selected. Prior to use, the rotating disk electrode was polished on a polishing machine, followed by cleaning the surface of the glassy carbon electrode. The catalyst ink was prepared as follows: 5 mg of the catalyst was first weighed into a 2 mL sample tube, to which 400 μL of ultrapure water, 550 μL of isopropanol, and 50 μL of Nafion solution were added. The sample tube was sealed and sonicated for 30 min in an ultrasonic bath. After removal, the corresponding amount of ink was pipetted onto the surface of the glassy carbon electrode, ensuring a platinum loading of 20 μg cm^{-2}.

During ink deposition, the rotation speed of the glassy carbon electrode was controlled at 100 rpm to ensure the catalyst formed a catalytic film on the electrode surface. The ink was allowed to air-dry naturally on the glassy carbon electrode surface to form a uniform catalytic layer.

All electrochemical measurements in this work were conducted on an electrochemical workstation (model 760E Bipotentiostat, CHI Instruments). The three-electrode testing system consisted of a reference electrode, a counter electrode, and a working electrode, corresponding to a saturated calomel electrode, a carbon rod, and a rotating disk electrode (RDE) loaded with catalyst, respectively. The electrolytes used were 0.1 M $HClO_4$ and a mixed solution of 0.1 M $HClO_4$ and 0.1 M H_3PO_4. Prior to testing, the electrode was wetted with deionized water to eliminate bubbles on the catalytic layer surface, ensuring no interference with the measurements.

For the ORR testing, the catalyst was first activated by performing multiple cyclic voltammetry (CV) scans within the potential range of –0.25 V to 0.73 V (vs. RHE) until the CV curves overlapped completely. The activation was carried out in N_2-saturated electrolyte at a rotation speed of 0 rpm. During ORR measurements, iR compensation (with a 90% compensation ratio) and background current subtraction were performed to evaluate the true catalytic activity accurately. The RDE measurements were conducted by linear sweep voltammetry (LSV) from 1.1 V to 0.05 V with a scan rate of 10 mV s^{-1} at 1600 rpm. The background current was obtained via linear sweep voltammetry in N_2-saturated electrolyte under the same rotation speed as the O_2-saturated tests, with continuous N_2 purging maintained.

3. High-temperature proton exchange membrane fuel cell measurements

A commercial 40 wt.% Pt/C catalyst was used as the anode catalyst, while the Pt@Mn-N-C catalyst served as the cathode catalyst. Catalyst inks were prepared using an identical procedure, with a mixed solvent of water and isopropanol (volume ratio 1:1). A diluted polytetrafluoroethylene (PTFE) emulsion was slowly added into the catalyst suspension, followed by magnetic stirring at 500 rpm for 10 min and ultrasonication for 15 min. This process was repeated three times to ensure uniform

dispersion.

The catalyst ink was sprayed onto carbon paper with a microporous layer by an air-spraying method to form electrodes with an area of 4 cm^2. The polybenzimidazole (PBI) membrane was dried at 100 ℃ for 1 h to remove residual solvent and moisture. The dried membrane (initial thickness: 40 μm) was then immersed in 85 wt.% phosphoric acid (PA) and treated at 150 ℃ for 40 min (final thickness after acid doping: 80 μm). After cooling to room temperature, excess PA on the membrane surface was removed. The acid doping level (ADL) was determined by a weighing method, yielding a value of 400%.

The cathode, PA-doped PBI membrane, and anode were hot-pressed at 160 ℃ and 1 MPa for 5 min to fabricate the membrane electrode assembly (MEA), with a compression ratio of 0.75. The MEA was assembled into a single cell using graphite flow fields, gaskets, and current collectors, with bolts tightened diagonally to 3.5 N·m. After confirming gas tightness, the cell was connected to the test station and heated to 160 ℃ for performance evaluation.

The Pt loading was controlled at 0.30 $mg_{Pt}·cm^{-2}$ for both the anode and cathode, with a binder content of 20 wt.% in the catalyst layer. HT-PEMFC tests were conducted at 160 °C under an H_2/O_2 atmosphere without backpressure. The stoichiometric ratios were set to 1.2 for the anode and 2.4 for the cathode, with gas flow rates of 0.1 $L·min^{-1}$. Polarization curves were recorded under steady-state conditions.

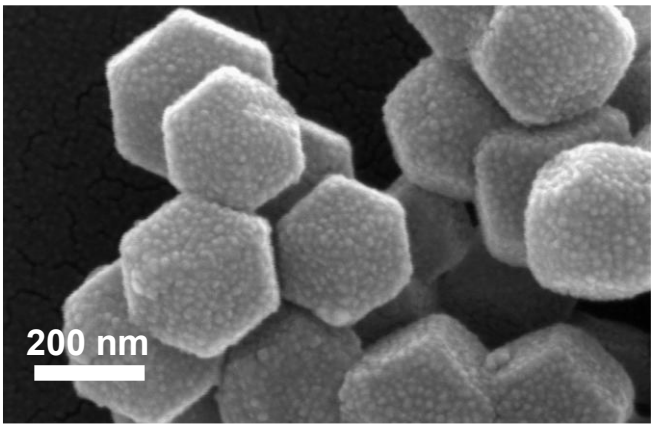

Figure S1. SEM image of Mn-N-C.

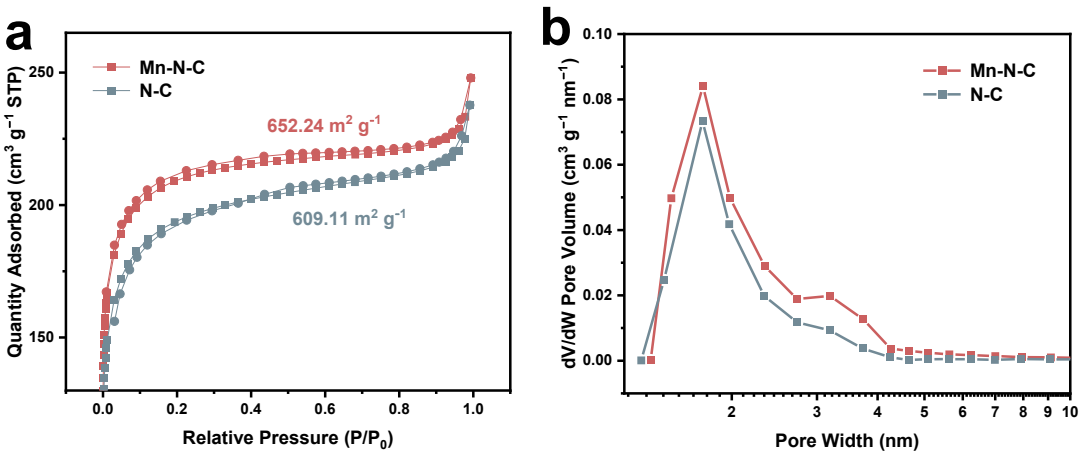

Figure S2. (a) N_2 adsorption-desorption isotherms. (b) The corresponding pore size distribution curves of Mn-N-C and N-C supports.

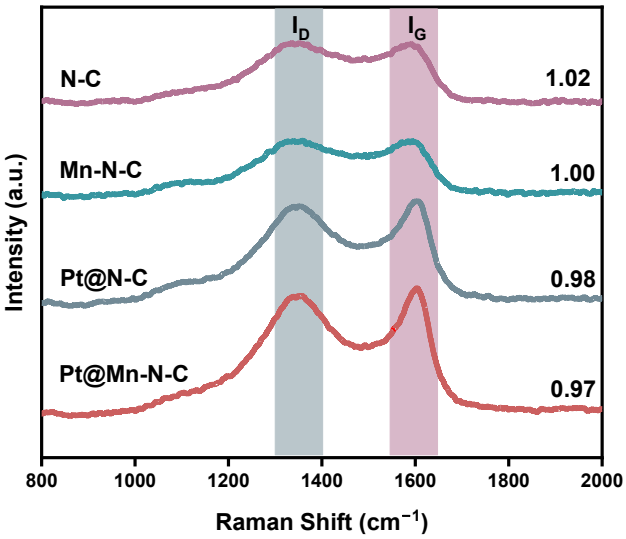

Figure S3. Raman spectra of N-C, Mn-N-C, Pt@N-C and Pt@Mn-N-C.

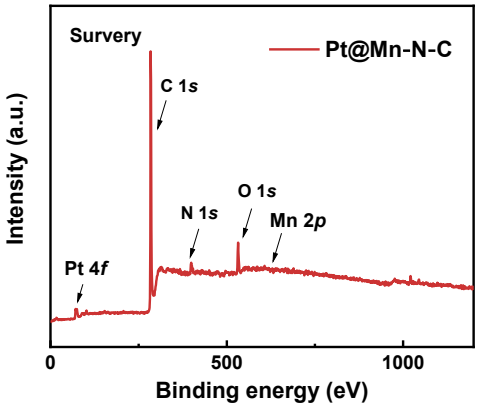

Figure S4. XPS survey of Pt@Mn-N-C.

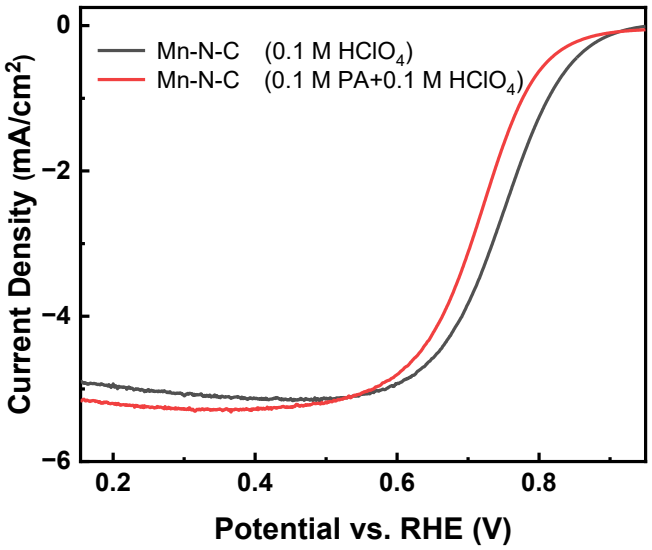

Figure S5. LSV curves of Mn-N-C in 0.1 M $HClO_4$ and 0.1 M PA + 0.1 M $HClO_4$.

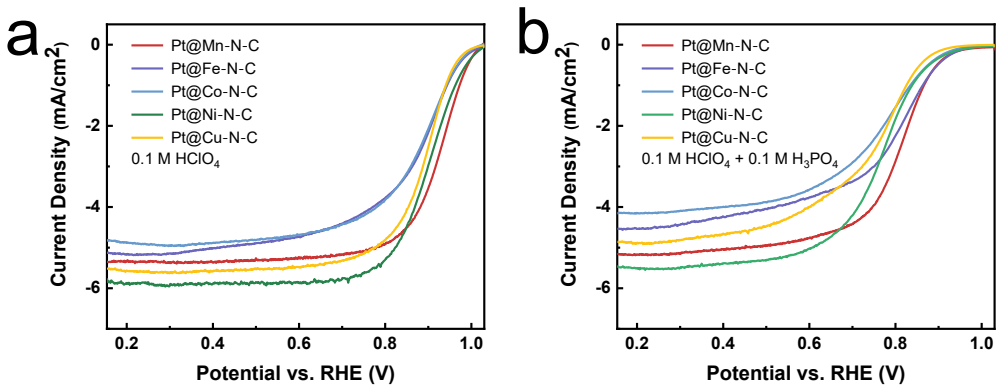

Figure S6. (a) LSV curves of Pt@M-N-C (M = Mn, Fe, Co, Ni, Cu) in 0.1 M $HClO_4$ electrolyte. (b) LSV curves of Pt@M-N-C (M = Mn, Fe, Co, Ni, Cu) in 0.1 M $HClO_4$ + 0.1 M PA electrolyte.

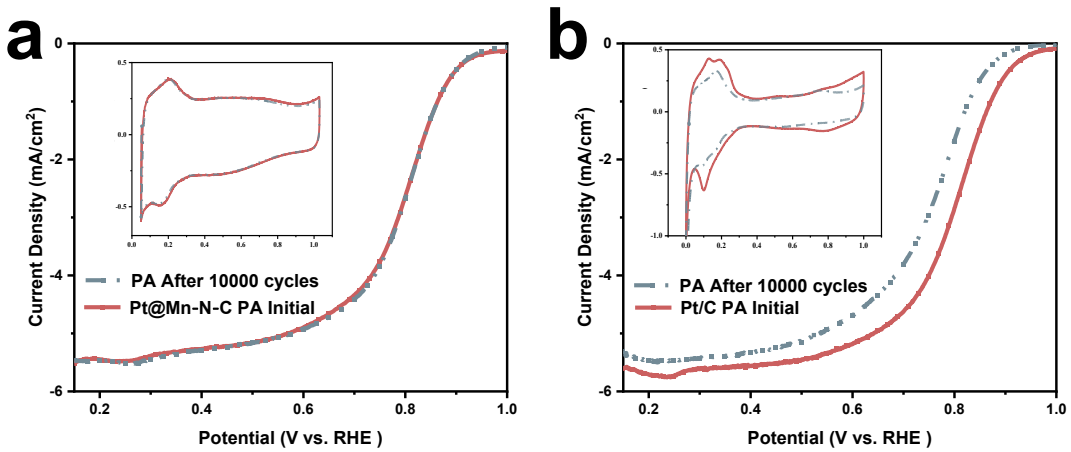

Figure S7. (a) Stability tests of Pt@Mn-N-C and (b) Pt/C in 0.1 M $HClO_4$ electrolyte.

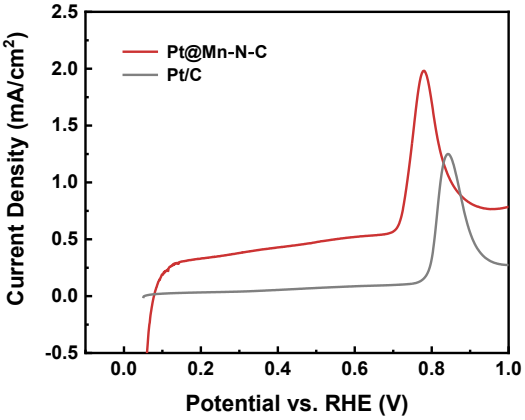

Figure S8. The electrochemical active surface areas of Pt@Mn-N-C and Pt/C were measured via the CO stripping method.

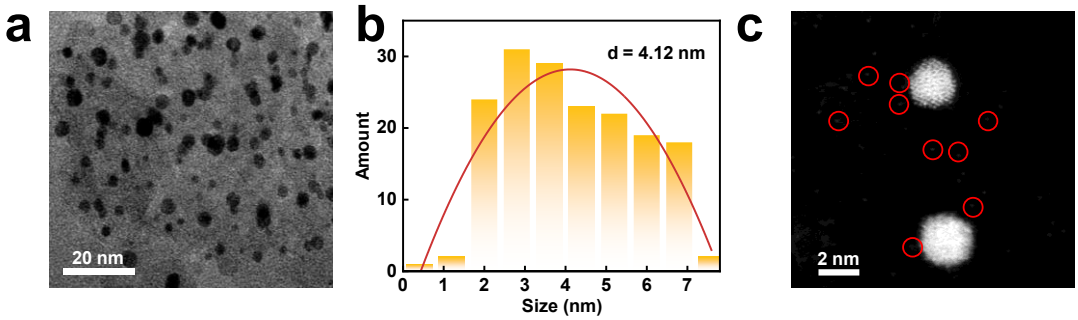

Figure S9. (a) TEM image of Pt@Mn-N-C after 10,000 cycles AST in 0.1 M $HClO_4$ + 0.1 M PA. (b) The size distribution diagram of Pt NPs. (c) AC-STEM image of Pt@Mn-N-C taken after 10,000 cycles AST in 0.1 M $HClO_4$ + 0.1 M PA.

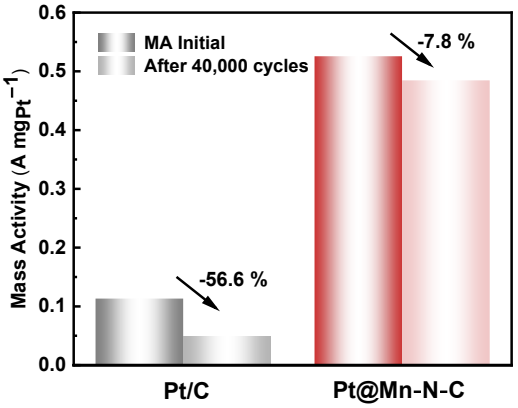

Figure S10. The MA comparison of Pt@Mn-N-C and Pt/C in O_2-saturated 0.1 M $HClO_4$ after 40,000 cycles AST.

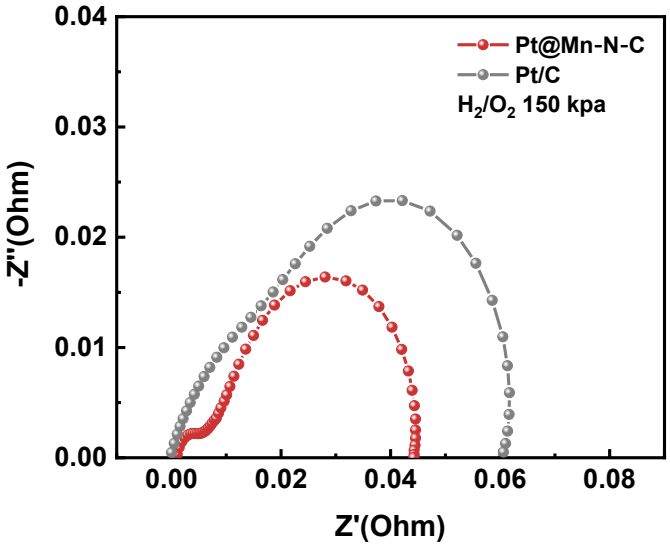

Figure S11. The Nyquist plots of EIS results.

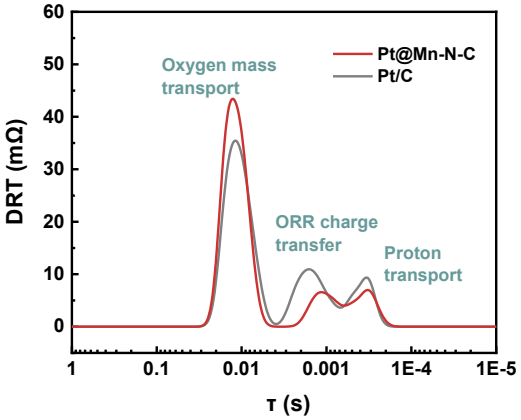

Figure S12. DRT plot obtained by deconvolving the EIS measurements.